

Molecular Structure and Magnetic Properties of μ -Oxo-bis[4-chloro-2,6-pyridinedicarboxylatodiaqua- iron(III)] Tetrahydrate, [Cl-C₇H₂NO₄(H₂O)₂Fe]₂O·4H₂O, a Complex with a Linear Fe₂O⁴⁺ Unit

Chia Chih Ou,^{1a} Ronald G. Wollmann,^{1b} David N. Hendrickson,^{*1b}
Joseph A. Potenza,^{*1a} and Harvey J. Schugar^{*1a}

Contribution from Wright & Rieman Chemistry Laboratories, Rutgers, The State University,
New Brunswick, New Jersey 08903, and the School of Chemical Sciences,
University of Illinois, Urbana, Illinois 61801. Received August 5, 1977

Abstract: The crystal and molecular structure of the title complex has been determined from single-crystal three-dimensional x-ray data collected by counter methods. [Cl-C₇H₂NO₄(H₂O)₂Fe]₂O·4H₂O crystallizes in space group C2/c (C_{2h}^6 , no. 15) with $Z = 4$, $a = 10.25$ (1), $b = 23.71$ (1), $c = 10.015$ (6) Å, $\beta = 90.0$ (1)°; $d_{\text{calcd}} = 1.831$, $d_{\text{obsd}} = 1.83$ (1) g/cm³. Least-squares refinement of 2405 reflections having $F^2 \geq 3\sigma(F^2)$ gave a conventional R factor of 0.049. The structure consists of discrete [Cl-C₇H₂NO₄(H₂O)₂Fe]₂O units with chemically (although not crystallographically) equivalent six-coordinate Fe(III) ions. Distorted octahedral NO₅ donor sets are composed of a bridging oxide ion, two water molecules, and a tridentate pyridinedicarboxylate ligand. Fe–O bond distances within the linear (crystallographically required) Fe₂O⁴⁺ unit are 1.773 (2) and 1.772 (3) Å and result in a Fe–Fe separation of 3.545 (1) Å. Magnetic susceptibility measurements show that the effective magnetic moment per Fe(III) gradually decreases from 1.94 μ_B at 270 K to 0.19 μ_B at 4.2 K. In the context of the $H = -2J\bar{S}_1\bar{S}_2$ spin–spin coupling model with g fixed at 2.0, the susceptibility data can be computer fitted with the parameters $-J = 115$ cm⁻¹ and TIP = 1.2×10^{-3} cgsu. An improved fit was obtained by incorporating a correction for 0.08% of an $S = \frac{5}{2}$ Fe(III) impurity, and yielded the parameters $-J = 107$ cm⁻¹, TIP = 8.5×10^{-4} cgsu. The extent of superexchange coupling in the title complex barely lies outside the range ($-J = 90$ – 100 cm⁻¹) reported for various bent ($\angle \text{Fe–O–Fe} = 139$ – 178 °) oxo-bridged Fe(III) dimers with nonheme ligands and Fe–O distances in the range 1.76–1.82 Å. The extent of superexchange coupling within Fe₂O⁴⁺ units is not a very sensitive function of the Fe–O–Fe bridging angle. More robust coupling ($-J = 122$ – 146 cm⁻¹) exhibited by various oxo-bridged Fe(III) heme dimers may be attributed in part to especially tight Fe–O bonding within their Fe₂O⁴⁺ units. Another possible contributing factor to these larger negative J values is the neglect of axial zero-field splitting in the Fe(III) heme units. Infrared spectra of the title complex are presented and discussed.

Introduction

Polynuclear complexes with two or more Fe(III) ions bridged by oxygen donor ligands play a central role in the inorganic and bioinorganic chemistry of the ferric ion.^{2,3} The simplest of these are dimeric species which contain either Fe₂O⁴⁺ or Fe₂(OH)₂⁴⁺ units. The relative ease of isolating oxo-bridged dimers in pure crystalline form has facilitated detailed characterization of the magnetic, electronic spectral, vibrational, and other features of the Fe₂O⁴⁺ unit.⁴ Oxo-bridged Fe(III) dimers display substantial antiferromagnetism which may be attributed to superexchange coupling of $S = \frac{5}{2}$ ferric ions via the oxo bridge. A series of such dimers differing in the coordination number of the Fe(III) ions (5–7), the chemical nature of the nonbridging ligands, and the Fe–O–Fe bridging angle (139–178°) all displayed a magnetochemistry well described by the $-2J\bar{S}_1\bar{S}_2$ exchange Hamiltonian with $\bar{S}_1 = \bar{S}_2 = \frac{5}{2}$, $-J = 90$ – 100 cm⁻¹, and $g = 2.0$. In contrast, various oxo-bridged Fe(III) heme dimers showed a significantly larger superexchange coupling ($-J = 122$ – 146 cm⁻¹).⁵ The source(s) of this enhanced antiferromagnetism has yet to be identified. The two heme dimers which have been studied crystallographically both contain nearly linear Fe₂O⁴⁺ units (Fe–O–Fe, 172–174.5°)^{5,6} and have relatively short Fe–O distances (≈ 1.73 – 1.763 (1) Å). The efficiency of antiferromagnetic superexchange in such systems depends on appropriate orbital overlap and is thought to maximize for a linear Fe–O–Fe bridge with tight Fe(III)–O bonding.⁷ Moreover, the enhanced antiferromagnetism of the heme dimers may reflect in some way the special electronic nature and structural restraints of the heme ligand. Accordingly, we have been interested in synthesizing a nonheme dimer with a linear Fe₂O⁴⁺ bridge so that the features of the 180° superexchange limit may be examined with “innocent” nonbridging ligands.

A second point of interest concerns the possible interconversion of Fe₂O⁴⁺ and Fe₂(OH)₂⁴⁺ dimers in solution, a process which was suggested in a kinetic study of the dissociation of an oxo-bridged Fe(III) complex.⁸ Evidence for the existence of both structural types has been presented for the aqueous Fe(III)-2,2'-6',2"-6",2"-tetrapyridyl system.⁹ The preparation and detailed characterization of Fe₂(OH)₂⁴⁺ dimers has proved to be surprisingly elusive, although recently a number of such dimers have been prepared in which the four non-bridging sites of each Fe(III) were occupied by a water molecule and by a terdentate pyridine-2,6-dicarboxylate ligand.¹⁰ To establish the effect of nonbridging ligands on the geometry and magnetic properties of the Fe₂(OH)₂⁴⁺ unit, substituent effects at the pyridine 4 position were investigated. Substituents such as –H, –OH, and –N(CH₃)₂ yielded Fe₂(OH)₂⁴⁺ dimers.^{10,11} In contrast, the Fe(III) complex of 4-chloro-2,6-pyridinedicarboxylate did not exhibit the O–H vibrational modes characteristic of Fe₂(OH)₂⁴⁺ complexes. The results of both infrared and magnetic measurements were consistent with a Fe₂O⁴⁺ structural unit. With a view toward comparing Fe₂O⁴⁺ and Fe₂(OH)₂⁴⁺ dimers with similar nonbridging ligands, we initiated a crystallographic study of the above oxo-bridged Fe(III) dimer. We report here the molecular structure of [Cl-C₇H₂NO₄(H₂O)₂Fe]₂O·4H₂O and the magnetic behavior of its linear Fe₂O⁴⁺ bridge. Issues raised above concerning the magnetism of oxo-bridged Fe(III) heme dimers are discussed in view of these results.

Experimental Section

(1) Preparation of [Cl-C₇H₂NO₄(H₂O)₂Fe]₂O·4H₂O. Chelidamic acid (Aldrich Chemical Co.) was converted by a published procedure¹² into either the dimethyl or diethyl ester of 4-chloropyridine-2,6-dicarboxylic acid. The free acid was prepared by saponification of the corresponding ester. The essentially water-insoluble title complex was

Table I. Crystal Data for $[\text{Cl}-\text{C}_7\text{H}_2\text{NO}_4(\text{H}_2\text{O})_2\text{Fe}]_2\text{O} \cdot 4\text{H}_2\text{O}$

$a, \text{\AA}$	10.25 (1)	Z	4
$b, \text{\AA}$	23.71 (1)	extinction	$hkl, h+k=2n+1, \text{and } h0l, l=2n+1$
$c, \text{\AA}$	10.015 (6)	space group	$C2/c$
β, deg	90.0 (1)	μ, cm^{-1}	15.3
$V, \text{\AA}^3$	2433.2	$\lambda, \text{\AA}$	0.710 69
$d_{\text{obsd}}, \text{g/cm}^3$	1.83 (1)	temp, $^\circ\text{C}$	22 \pm 1
$d_{\text{calcd}}, \text{g/cm}^3$	1.831	mol wt	670.9

prepared in crystalline form by the urea hydrolysis technique.¹⁰ Several experiments indicated that preparations employing either diester yielded better crystals than preparations employing the free diacid. In a typical preparation, 2.5 mmol each of diester, $\text{FeCl}_3 \cdot 6\text{H}_2\text{O}$, and urea were dissolved in 150 mL of hot ($\sim 80^\circ\text{C}$), distilled H_2O . The resulting light brown solution was filtered through a 0.22- μm pore size membrane filter and placed in an oven maintained at $90 \pm 1^\circ\text{C}$. After 1 day, a finely divided yellow precipitate and dark brown aqueous phase were obtained. Over an additional 2-day period, the yellow precipitate gradually disappeared while red-brown crystals of the title complex grew. The product was collected by filtration, washed with distilled H_2O , and dried in air at room temperature. The yield was 0.80 g (96%).

Anal. Calcd for $\text{Fe}_2\text{C}_{14}\text{H}_{20}\text{N}_2\text{O}_{17}\text{Cl}_2$: Fe, 16.65; C, 25.06; H, 3.01; N, 4.18; Cl, 10.57. Found: Fe, 16.50 (iodometry); C, 24.80; H, 3.26; N, 4.12; Cl, 10.75.

Examination of the chunky plates with a polarizing microscope revealed that the major face was not significantly dichroic. Moreover, for nearly all of the sample, the extinctions of this face varied from partial to approximately zero. However, a few crystals were obtained that did exhibit sharp extinctions; one of these was used to collect diffraction data.

(2) **Physical Measurements.** Infrared spectra were recorded using Perkin-Elmer Models 467 and 225 spectrophotometers. Samples were dispersed in 13-mm diameter KBr pellets. Low-temperature spectra were obtained using a cryocooling head equipped with KBr windows and a Cryogenic Technology Inc. "Spectrum" closed-cycle helium gas refrigerator. As previously described,¹³ temperatures in the 20–30 K range were obtainable. Spectral studies of the title complex as single crystals, mulls, and pressed (neat) disks were made with a Cary 14 spectrophotometer.

Magnetic susceptibility data over the 4.2–270 K temperature range were obtained with a Princeton Applied Research Model 150 A vibrating-sample magnetometer. Temperatures were monitored by using a GaAs diode in conjunction with a $\text{CuSO}_4 \cdot 5\text{H}_2\text{O}$ standard. Computer fitting of the magnetic susceptibility data was performed on an IBM 360/75 computer and utilized an adapted version of the function minimization program STEPT.¹⁴

(3) **Collection of Diffraction Data.** A crystal of dimensions $0.55 \times 0.15 \times 0.35$ mm was mounted on the end of a glass rod along a face diagonal (a axis). Preliminary Weissenberg and precession photographs revealed systematic absences for $hkl, h+k=2n+1$, and $h0l, l=2n+1$. From visual examination, the photographs appeared to have mmm Laue symmetry; therefore, we assumed the complex to have crystallized in an orthorhombic unit cell. After we attempted unsuccessfully to solve the structure in the orthorhombic space groups consistent with these observations ($Cmcm$, D_{2h}^{17} , no. 63; $Ama2$, C_{2h}^{16} , no. 40; $Cmc2_1$, C_{2h}^{12} , no. 36), the symmetry of the reciprocal lattice was examined carefully using an Enraf-Nonius CAD-3 automated diffractometer. This examination revealed a monoclinic (Laue symmetry $2/m$) pseudoorthorhombic cell with $\beta = 90.0 (1)^\circ$. As an example of the extent of the deviation from mmm symmetry, we cite the percent difference between $|F_{hkl}|$ and $|F_{h\bar{k}\bar{l}}|$, which was found to be 31%. The structure was solved and refined successfully in space group $C2/c$ (C_{2h}^8 , no. 15), which is consistent with the observed systematic absence and reciprocal lattice symmetry.

Unit cell dimensions (Table I) were determined from a least-squares fit of the θ , χ , and ϕ values of 13 reflections obtained using graphite monochromated Mo $\text{K}\alpha$ radiation ($\lambda = 0.710\ 69\ \text{\AA}$) and an Enraf-Nonius CAD-3 automated diffractometer. The crystal density was measured by the gradient method¹⁵ using tetrabromothiane as the high-density medium and CH_2Cl_2 as the low-density medium; $\text{CoCl}_2 \cdot 6\text{H}_2\text{O}$ ($d = 1.924\ \text{g/cm}^3$), $\text{Fe}(\text{NH}_4)_2(\text{SO}_4)_2 \cdot 6\text{H}_2\text{O}$ ($d = 1.864$

g/cm^3), and $(\text{NH}_4)_2\text{SO}_4$ ($d = [769\ \text{G/cm}^3]$) were used as standards.¹⁶ The observed value of $1.83 (1)\ \text{g/cm}^3$ agreed well with the value of $1.831\ \text{g/cm}^3$ calculated for four $[\text{Cl}-\text{C}_7\text{H}_2\text{NO}_4(\text{H}_2\text{O})_2\text{Fe}]_2 \cdot 4\text{H}_2\text{O}$ units per unit cell.

A θ - 2θ scan ($2^\circ < \theta < 30^\circ$) was used to collect 4050 unique reflections covering one quadrant ($+h, +k, \pm l$) of reciprocal space. Of these, 1271 in the $+h, +k, +l$ octant with $F^2 > 3\sigma(F^2)$ were used in an attempt to obtain a trial structure in an orthorhombic space group. Later, 2405 reflections with $F^2 > 3\sigma(F^2)$ and indexes $+h, +k, \pm l$ were used to refine the structure in space group $C2/c$. All diffraction data were corrected for Lorentz, polarization, and absorption effects. Transmission factors ranged from 0.57 to 0.79 using a linear absorption coefficient of $15.3\ \text{cm}^{-1}$ for Mo $\text{K}\alpha$ radiation. Additional aspects of the data collection process have been described elsewhere.¹⁷

(4) **Solution and Refinement of the Structure.**¹⁸ The structure was solved by the heavy atom method and refined using full-matrix least-squares techniques. Space group $Cmcm$ was assumed initially. Analysis of a normal sharpened Patterson map revealed the two unique iron and two unique chlorine atoms at special position $4c(0, y, 1/4)$. Five additional atoms (Ox, N(1), N(2), C(7), and C(8)) were located by a series of structure factor, difference Fourier calculations, and all were found to occupy $4c$ sites. Thus, these nine atoms were located on a line. Use of these atoms for a structure factor calculation gave a rather high value of $R_F = \sum |F_o| - |F_c| / \sum |F_o| = 0.45$. Although further phasing proved difficult, coordinates for two of the ring carbon atoms (C(1) and C(4)) were eventually determined.

At this point, it became apparent that the true space group could not be $Cmcm$, $Cmc2_1$, or $Ama2$. Each of these has mirror planes perpendicular to a and/or c , and the location of nine atoms on the line $(0, y, 1/4)$ would require the oxy-bridged dimer to have m or mm symmetry. Enforcing this mirror symmetry proved difficult and unrewarding, and so we assumed that the dimer probably had point symmetry 2.

Since we still thought that the structure was orthorhombic and that point symmetry 2 was required, space group $C22_1$ was assumed (note that $C22_1$ is not consistent with the glide plane extinction). A series of structure factor, difference Fourier calculations revealed coordinates for all remaining nonhydrogen atoms except those of the lattice water molecules. The value of $R_F (0.41)$ was still unusually high. Inspection of intermolecular distances revealed that (calculated) hydrogen atoms from two symmetry-related pyridinedicarboxylate ligands were too close. To remedy this, one ligand would have to be rotated, destroying the orthorhombic symmetry. This led us to reexamine the reciprocal lattice (vide supra) and finally to space group $C2/c$ with $\beta = 90.0 (1)^\circ$ in which the remaining nonhydrogen atoms were easily located.

Initial refinement was based on F^2 and weights were set according to $w = 1/\sigma^2(F^2)$. Neutral atom scattering factors were obtained from Cromer and Waber.¹⁹ Real and imaginary parts of the anomalous dispersion correction²⁰ were applied to iron and chlorine. Several cycles of isotropic refinement reduced R_F to 0.095; three additional cycles utilizing anisotropic thermal parameters reduced R_F to 0.061.

At this stage, hydrogen atoms were located on a difference Fourier map and added as a fixed atom contribution to the structure factor with isotropic temperature factors equal to those of the atoms to which they are attached. Further refinement was based on F . A weighting scheme, chosen by an analysis of variance, led to the following assignments for $\sigma(F_o)$:

$$\sigma(F_o) = 1.366 - 0.0064|F_o|, |F_o| \leq 16.9$$

$$\sigma(F_o) = 0.344 + 0.054|F_o|, |F_o| > 16.9$$

Several additional cycles of anisotropic refinement led to convergence with $R_F = 0.049$ and $R_{wF} = [\sum w(F_o - F_c)^2 / \sum wF_o^2]^{1/2} = 0.068$. For the final cycle, all parameter changes were less than their associated esd's. A final difference electron density map showed a general background of $\pm 0.3\ \text{e}/\text{\AA}^3$ and revealed no significant features. Final atomic parameters, together with their estimated standard deviations, are given in Table II. A view of the structure, showing the atom numbering scheme, is given in Figure 1. A list of observed and calculated structure factors is available.²¹

Lastly, we mention that an attempt was made to refine the structure in space group Cc which is also consistent with the observed diffraction pattern and which would permit an Fe-O-Fe bond angle different

Table II. Fractional Atomic Coordinates^a and Thermal Parameters^b for [Cl-C₇H₂NO₄(H₂O)₂Fe]₂O·4H₂O

atom	x	y	z	β_{11} or $B, \text{Å}^2$	β_{22}	β_{33}	β_{12}	β_{13}	β_{23}
Fe(1)	0	1751.7 (2)	1/4	26.2 (4)	2.5 (1)	30.5 (5)	0	-3.2 (4)	0
Fe(2)	0	3246.9 (2)	1/4	23.1 (4)	2.4 (1)	33.2 (5)	0	-3.6 (4)	0
Cl(1)	0	-1005.4 (5)	1/4	88.0 (13)	3.1 (2)	84.3 (14)	0	-3.9 (12)	0
Cl(2)	0	6002.3 (5)	1/4	86.6 (13)	2.9 (2)	102.4 (15)	0	5.2 (13)	0
Ox	0	2500 (1)	1/4	51 (3)	3.3 (4)	55 (3)	0	-3 (2)	0
O(1)	1206 (2)	1515 (1)	4092 (2)	52 (2)	3.7 (3)	50 (2)	2(1)	25 (2)	-2 (1)
O(2)	2266 (2)	811 (1)	5094 (2)	48 (2)	6.6 (4)	57 (2)	4(1)	30 (2)	-2 (1)
O(3)	1578 (2)	1713 (1)	1239 (3)	47 (2)	7.1 (4)	83 (3)	-5(1)	30 (2)	-9 (1)
O(4)	1433 (2)	3480 (1)	1116 (2)	45 (2)	4.1 (3)	53 (2)	1(1)	13 (2)	1 (1)
O(5)	2326 (2)	4186 (1)	-37 (2)	51 (2)	6.7 (4)	58 (2)	-5(1)	23 (2)	-4 (1)
O(6)	1392 (3)	3283 (1)	3979 (3)	60 (2)	8.6 (4)	59 (3)	-6(1)	-35 (2)	3 (1)
O(7)	3260 (3)	2578 (1)	1576 (3)	49 (2)	9.3 (4)	66 (2)	0(1)	-2 (2)	3 (1)
O(8)	4101 (3)	2549 (1)	4232 (3)	61 (2)	10.0 (4)	53 (2)	3(1)	-9 (2)	-1 (1)
N(1)	0	863 (1)	1/4	32 (3)	1.8 (5)	38 (3)	0	-11 (3)	0
N(2)	0	4134 (1)	1/4	37 (3)	1.9 (5)	37 (3)	0	4 (3)	0
C(1)	722 (3)	593 (1)	3390 (3)	30 (2)	3.6 (4)	38 (2)	2(1)	-8 (2)	-1 (1)
C(2)	754 (3)	10 (1)	3434 (3)	45 (3)	3.9 (4)	46 (3)	3(1)	-8 (2)	3 (1)
C(3)	1478 (3)	997 (1)	4283 (3)	33 (2)	4.3 (4)	37 (2)	1(1)	-9 (2)	-2 (1)
C(4)	774 (3)	4406 (1)	1651 (3)	28 (2)	4.4 (4)	36 (2)	-2(1)	3 (2)	0 (1)
C(5)	788 (3)	4990 (1)	1594 (3)	40 (3)	4.3 (4)	46 (3)	-2(1)	0 (2)	3 (1)
C(6)	1589 (3)	4000 (1)	825 (3)	31 (2)	4.4 (4)	39 (3)	-2(1)	1 (2)	-3 (1)
C(7)	0	-277 (2)	1/4	50 (4)	3.1 (6)	49 (4)	0	4 (3)	0
C(8)	0	5274 (2)	1/4	47 (4)	3.1 (6)	60 (4)	0	-6 (4)	0
H(C2)	119	-18	403	1.82					
H(C5)	126	517	97	1.70					
H(O3-1)	217	199	136	1.91					
H(O3-2)	205	143	80	1.91					
H(O6-1)	120	300	453	2.18					
H(O6-2)	182	354	428	2.18					
H(O7-1)	297	292	133	2.52					
H(O7-2)	407	259	130	2.52					
H(O8-1)	400	290	456	2.54					
H(O8-2)	382	262	337	2.54					

^a Nonhydrogen coordinates are $\times 10^4$; hydrogen coordinates are $\times 10^3$. ^b Anisotropic thermal parameters are $\times 10^4$; the form of the anisotropic thermal ellipsoid is $\exp[-(\beta_{11}h^2 + \beta_{22}k^2 + \beta_{33}l^2 + 2\beta_{12}hk + 2\beta_{13}hl + 2\beta_{23}kl)]$.

from 180°. Beginning with the final parameters for space group *C*2/c, block refinement was performed on parameters not related by the twofold axis in *C*2/c (full-matrix refinement gave singular matrices). Although this procedure eventually reduced *R*_{wF} to 0.066 and the Fe-O-Fe angle to ~178°, subsequent attempts at full-matrix refinement still gave singular matrices. We conclude that, within the limitations of the least-squares refinement, the molecule contains a twofold axis in space group *C*2/c. This view is also supported by the excellent agreement between chemically related interatomic distances (Table III), by the orientations of the thermal ellipsoids which are approximately normal to bond axes (Figure 1), and by the root mean square values of the thermal displacements along the principal axes of the ellipsoids which vary from 0.07 to 0.23 Å for the entire molecule.

Description of the Structure

The structure consists of discrete [Cl-C₇H₂NO₄(H₂O)₂-Fe]₂O dimeric units with point symmetry 2. Each unit contains two chemically (although not crystallographically) equivalent, six-coordinate Fe(III) ions. The distorted octahedral NO₅ donor sets are composed of a bridging oxide ion, two water molecules, and a terdentate pyridinedicarboxylate ligand. Owing to the limited ligand bite, the O(1)-Fe(1)-O(1') and O(4)-Fe(2)-O(4') bond angles (Table III) are reduced from their idealized value of 180° to 148.9 (1) and 149.4 (1)°, respectively. This structural feature has been observed previously with three Fe₂(OH)₂⁴⁺ dimers containing different pyridine-2,6-dicarboxylate ligands.^{10,11} Nine atoms (Cl(1), C(7), N(1), Fe(1), Ox, Fe(2), N(2), C(8), and Cl(2)) lie along a crystallographic twofold axis (0, *y*, 1/4). Thus, the Fe-O-Fe bridging angle crystallographically is constrained to be 180°. The Fe-Ox distances [1.773 (2) and 1.772 (3) Å] are equiv-

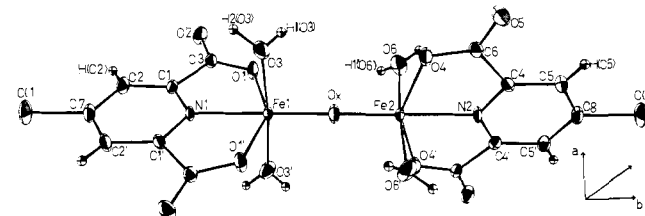


Figure 1. Molecular structure of [Cl-C₇H₂NO₄(H₂O)₂Fe]₂O·4H₂O showing the atom numbering scheme. Lattice water molecules have been omitted for clarity.

alent and lie in the middle of the range reported for other Fe₂O⁴⁺ complexes (1.73–1.82 Å).^{4–6} As noted for other Fe₂O⁴⁺ complexes, the Fe-O bonds in the bridge are significantly shorter than both the Fe-O(H₂O) bonds [2.053 (3), 2.058 (3) Å] and the Fe-O(carboxylate) bonds [2.094 (2), 2.093 (2) Å]. The Fe-N distances (2.107 (3) and 2.102 (3) Å) are the longest yet observed in dimeric Fe(III) complexes of 4-substituted pyridine-2,6-dicarboxylates. In a series of three Fe₂(OH)₂⁴⁺ dimers with the 4 substituents -N(CH₃)₂, -OH, and -H, the respective Fe-N distances were observed^{10,11} to be 2.043 (6), 2.057 (5), and 2.070 (6) Å. This increase in the Fe-N bond length may be associated with the accompanying decrease in ligand basicities (i.e., electron density on the pyridine nitrogen atom) known from titration studies²² and is in harmony with the Hammett constants²³ of the substituents. A further diminution in ligand basicity (and therefore increase in Fe-N bond length) is expected for the 4-chloro derivative.

Table III. Bond Distances (Å) and Angles (deg) for $[Cl-C_7H_2NO_4(H_2O)_2Fe]_2\cdot 4H_2O$

atoms	distance	atoms	distance
Fe(1)-Ox	1.773 (3)	Fe(2)-Ox	1.772 (3)
Fe(1)-O(1)	2.094 (2)	Fe(2)-O(4)	2.093 (2)
Fe(1)-O(3)	2.053 (3)	Fe(2)-O(6)	2.058 (3)
Fe(1)-N(1)	2.107 (3)	Fe(2)-N(2)	2.102 (3)
Fe(1)...Fe(2)	3.545 (1)		
N(1)-C(1)	1.324 (3)	N(2)-C(4)	1.330 (4)
C(1)-C(2)	1.384 (4)	C(4)-C(5)	1.384 (4)
C(2)-C(7)	1.390 (4)	C(5)-C(8)	1.389 (4)
C(7)-Cl(1)	1.728 (5)	C(8)-Cl(2)	1.728 (5)
C(1)-C(3)	1.523 (4)	C(4)-C(6)	1.520 (4)
C(3)-O(1)	1.273 (4)	C(6)-O(4)	1.278 (4)
C(3)-O(2)	1.228 (4)	C(6)-O(5)	1.229 (4)
atoms	angle	atoms	angle
Ox-Fe(1)-O(1)	105.5 (1)	Ox-Fe(2)-O(4)	105.3 (1)
Ox-Fe(1)-N(1)	180	Ox-Fe(2)-N(2)	180
Ox-Fe(1)-O(3)	92.5 (1)	Ox-Fe(2)-O(6)	92.4 (1)
N(1)-Fe(1)-O(3)	87.5 (1)	N(2)-Fe(2)-O(6)	87.6 (1)
N(1)-Fe(1)-O(1)	74.5 (1)	N(2)-Fe(2)-O(4)	74.7 (1)
O(3)-Fe(1)-O(1)	89.5 (1)	O(6)-Fe(2)-O(4)	88.8 (1)
O(3)-Fe(1)-O(3')	174.9 (1)	O(6)-Fe(2)-O(6')	175.3 (1)
O(1)-Fe(1)-O(3')	89.1 (1)	O(4)-Fe(2)-O(6')	89.9 (1)
O(1)-Fe(1)-O(1')	148.9 (1)	O(4)-Fe(2)-O(4')	149.4 (1)
Fe(1)-Ox-Fe(2)	180		
Fe(1)-N(1)-C(1)	119.0 (2)	Fe(2)-N(2)-C(4)	119.1 (2)
Fe(1)-O(1)-C(3)	120.1 (2)	Fe(2)-O(4)-C(6)	119.6 (2)
C(1)-N(1)-C(1')	122.1 (4)	C(4)-N(2)-C(4')	121.9 (4)
N(1)-C(1)-C(2)	122.2 (3)	N(2)-C(4)-C(5)	121.2 (3)
N(1)-C(1)-C(3)	112.0 (3)	N(2)-C(4)-C(6)	111.6 (3)
C(1)-C(2)-C(7)	117.0 (3)	C(4)-C(5)-C(8)	116.8 (3)
C(2)-C(7)-C(2')	121.5 (4)	C(5)-C(8)-C(5')	122.0 (4)
C(2)-C(7)-Cl(1)	119.2 (2)	C(5)-C(8)-Cl(2)	119.0 (2)
C(1)-C(3)-O(2)	119.8 (3)	C(4)-C(6)-O(5)	119.6 (3)
C(1)-C(3)-O(1)	114.1 (3)	C(4)-C(6)-O(4)	114.8 (3)
O(1)-C(3)-O(2)	126.1 (3)	O(4)-C(6)-O(5)	125.7 (3)

The relatively long Fe-N bond distances observed for the title complex may in part also be due to a trans effect. The Fe-N bonds in the dihydroxy dimers are trans to the bridging OH groups whereas those in the title complex are trans to the more tightly bound bridging oxide groups. Except for the features of the Fe-N and Fe-Ox bonds noted above, the remaining Fe(III) bond distances are comparable to those observed for related $Fe_2(OH)_2^{4+}$ dimers.^{10,11} The remaining four Fe(III) bonds to the various oxygen donors (carboxylate, H_2O , OH) in the title complex and in the three related $Fe_2(OH)_2^{4+}$ complexes fall in the 1.99–2.09 Å range, which is typical for Fe(III)-O bonds in complexes of $S = \frac{5}{2}$ Fe(III).²⁴

Bond distances and angles within the terdentate ligand are unremarkable and compare closely with those observed for structures with chemically similar ligands. The pyridine ring units are planar to approximately ± 0.01 Å while the carboxylate groups are bent and twisted slightly from these planes (Table IV). Unique to this particular terdentate ligand are the C-Cl bond lengths, both of which are 1.728 (5) Å. These distances are close to those reported for other C(aromatic)-Cl bonds.²⁵ Overall, we note that structural parameters for both halves of the dimer are identical within experimental error, indicating that refinement of the structure was reliable.

In the crystal, dimers are linked together loosely by an extensive hydrogen bonding network involving the bridging oxide ion, the carboxylate oxygen atoms, and both ligand and lattice water molecules. Inter- and intramolecular hydrogen bonding distances are presented in Table V. Both the hydrogen bonding network and the packing of the structure are shown in Figure 2.

Magnetic Susceptibility Results and Discussion

A diamagnetism of -350×10^{-6} cgsu was estimated for the dimer, using Pascal's constants.²⁶ Corrected magnetic susceptibilities per mol of dimer (χ_M) are listed in Table VI and plotted in Figure 3. Effective magnetic moments (μ_{eff}) per Fe(III) were calculated from the corrected susceptibility data using the formula $\mu_{eff}^2 = (7.998/2)\chi_M T$. An antiferromagnetic exchange interaction clearly is indicated by the gradual decrease of μ_{eff} from 1.91 μ_B at 270 K to 0.19 μ_B at 4.2 K.

The expression for χ_M employing the usual spin-spin interaction model based upon the exchange Hamiltonian $H = -2J\bar{S}_1\bar{S}_2$ with $S_1 = S_2 = \frac{5}{2}$ has been derived elsewhere.^{26,27} Inclusion of terms for the temperature-independent paramagnetic susceptibility (TIP) and for possible sample contamination by a paramagnetic Fe(III) monomeric impurity ($4.4T^{-1}\chi_{para}$) yields the relationship

$$\chi_M = \frac{2Ng^2\beta^2}{kT} \left(\frac{55 + 30z^{10} + 14z^{18} + 5z^{24} + z^{28}}{11 + 9z^{10} + 7z^{18} + 5z^{24} + 3z^{28} + z^{30}} \right) + \frac{4.4\chi_{para}}{T} + TIP$$

where $z = \exp[-J/kT]$ and N , g , β , k , and T have their usual meanings.

A least-squares fitting computer program was used to fit the observed data to the above equation for two different cases. First, g was assumed to be 2.00 and contamination by a paramagnetic Fe(III) monomer was ignored; the computer fit yielded $-J = 115 \text{ cm}^{-1}$ and TIP = 1.2×10^{-3} cgsu. Second, g was assumed to be 2.00 and the impurity term was included.

Table IV. Least-Squares Planes and Deviations Therefrom for [Cl-C₇H₂NO₄(H₂O)₂Fe]₂O·4H₂O

plane	A	B	C	D	Equations of the Planes ^{a,b}			
					atoms defining plane			
I	-0.7703	0.0	0.6377	1.5965	N(1), C(1), C(2), C(7), Cl(1), C(2'), ^c C(1')			
II	0.7396	0.0	0.6730	1.6850	N(2), C(4), C(5), C(8), Cl(2), C(5'), C(4')			
III	-0.7590	0.0	0.6511	1.6301	N(1), C(1), C(2), C(7), Cl(1), C(2'), C(1'), C(3), O(1), O(2), C(3'), O(1'), O(2')			
IV	0.7203	0.0	0.6937	1.7369	N(2), C(4), C(5), C(8), Cl(2), C(5'), C(4'), C(6), O(4), O(5), O(6'), O(4'), O(5')			
V	-0.8502	0.5163	0.1033	2.2341	O(1), O(1'), O(3), O(3')			
VI	0.9672	0.0	0.2538	0.6355	O(4), O(4'), O(6), O(6')			
Deviations from the Planes								
		atom	dev, Å		atom	dev, Å		
I		N(1)	0.0		II	N(2)	0.0	
		C(1)	-0.0015			C(4)	0.0144	
		C(2)	0.0013			C(5)	-0.0134	
		C(7)	0.0			C(8)	0.0	
		Cl(1)	0.0			Cl(2)	0.0	
		C(2')	-0.0013			C(5')	0.0134	
		C(1')	0.0015			C(4')	-0.0144	
		Fe	0.0			Fe(2)	0.0	
III		N(1)	0.0		IV	N(2)	0.0	
		C(1)	0.0188			C(4)	-0.0186	
		C(2)	0.0226			C(5)	-0.0479	
		C(7)	0.0			C(8)	0.0	
		Cl(1)	0.0			Cl(2)	0.0	
		C(2')	-0.0226			C(5')	0.0479	
		C(1')	-0.0188			C(4')	0.0186	
		C(3)	0.0130			C(6)	0.0090	
		O(1)	0.1000			O(4)	0.0961	
		O(2)	-0.0711			O(5)	-0.0459	
		C(3')	-0.0130			C(6')	-0.0090	
		O(1')	-0.1000			O(4')	-0.0961	
		O(2')	0.0711			O(5')	0.0459	
		Fe(1)	0.0			Fe(2)	0.0	
V		O(1)	-1.007		VI	O(4)	1.068	
		O(1')	0.7648			O(4')	-1.068	
		O(3)	-1.384			O(6)	1.756	
		O(3')	1.626			O(6')	-1.756	
		Fe(1)	0.1686			Fe(2)	0.0	

^a Equations are of the form $AX_0 + BY_0 + CZ_0 = D$ where X_0 , Y_0 , and Z_0 are Cartesian axes lying along bxc^* , b , and c^* , respectively. ^b The following sets of atoms are strictly coplanar: Ox, N(1), O(1), O(1'), Fe(1); Ox, N(2), O(4), O(4'), Fe(2); Ox, N(1), O(3), O(3'), Fe(1); Ox, N(2), O(6), O(6'), Fe(2). ^c Corresponding primed and unprimed atoms are related by a twofold axis along b .

Table V. Hydrogen Bonding Contacts in [Cl-C₇H₂NO₄(H₂O)₂Fe]₂O·4H₂O

donor (D)	hydrogen (H)	acceptor (A) ^a	D-H...A	D...A	H...A ^b
O(3)	H(O3-1)	O(7) (i)	176	2.699	1.80
O(3)	H(O3-2)	O(5) (ii)	169	2.693	1.77
O(6)	H(O6-1)	O(8) (iii)	175	2.712	1.82
O(6)	H(O6-2)	O(2) (iii)	175	2.713	1.91
O(7)	H(O7-1)	O(4) (i)	149	2.880	2.07
O(7)	H(O7-2)	O(8) (iv)	175	2.823	1.95
O(8)	H(O8-1)	O(1) (iii)	157	2.800	1.95
O(8)	H(O8-2)	O(7) (i)	167	2.798	1.89
O(3)	H(O3-1)	Ox (i)	81	2.772	2.78
O(3)	H(O3-2)	O(4) (ii)	129	3.151	2.48
O(6)	H(O6-1)	Ox (i)	88	2.711	2.65
O(6)	H(O6-2)	O(1) (iii)	129	3.165	2.60
O(6)	H(O6-2)	N(2) (i)	78	2.880	2.94
O(7)	H(O7-1)	O(3) (ii)	119	3.286	2.76
O(7)	H(O7-2)	O(8) (i)	72	2.798	2.94
O(8)	H(O8-1)	O(6) (i)	119	3.286	2.88
C(2)	H(C2)	O(5) (v)	162	3.204	2.37
C(2)	H(C2)	Cl(1) (i)	76	2.695	2.77
C(2)	H(C2)	O(2) (i)	92	2.963	2.80
C(5)	H(C5)	O(2) (vi)	162	3.260	2.40
C(5)	H(C5)	O(5) (i)	94	2.964	2.77
C(5)	H(C5)	Cl(2) (i)	73	2.691	2.81

^a Numbers in parentheses indicate the following symmetry transformations: i = x, y, z ; ii = $\frac{1}{2} - x, \frac{1}{2} - y, z$; iii = $\frac{1}{2} - x, \frac{1}{2} - y, 1 - z$; iv = $1 - x, y, \frac{1}{2} - z$; v = $\frac{1}{2} - x, -\frac{1}{2} + y, \frac{1}{2} - z$; vi = $\frac{1}{2} - x, \frac{1}{2} + y, \frac{1}{2} - z$. ^b Only H...A distances less than 3 Å are listed.

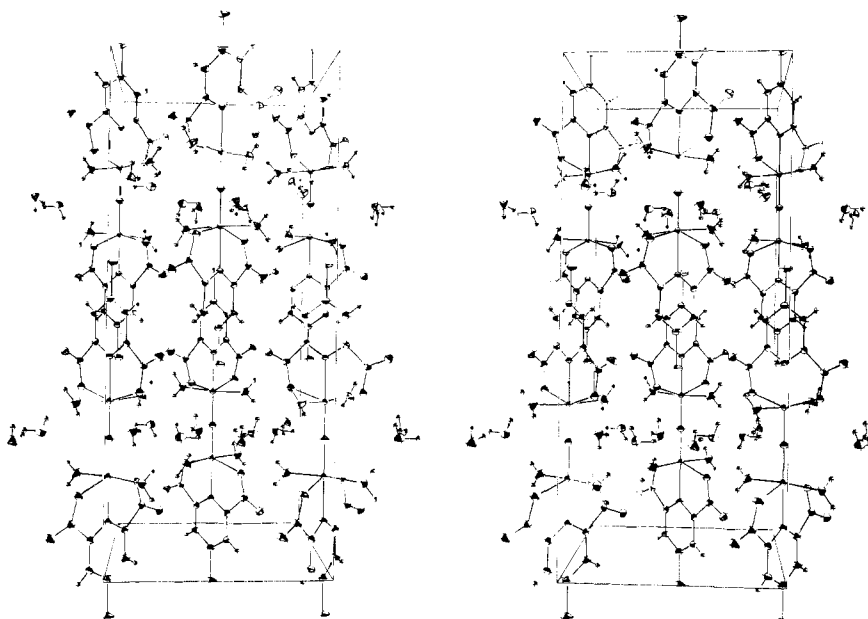


Figure 2. Stereoscopic packing diagram of $[\text{Cl}-\text{C}_7\text{H}_2\text{NO}_4(\text{H}_2\text{O})_2\text{Fe}]_2\text{O} \cdot 4\text{H}_2\text{O}$ showing the hydrogen bonding network (light lines).

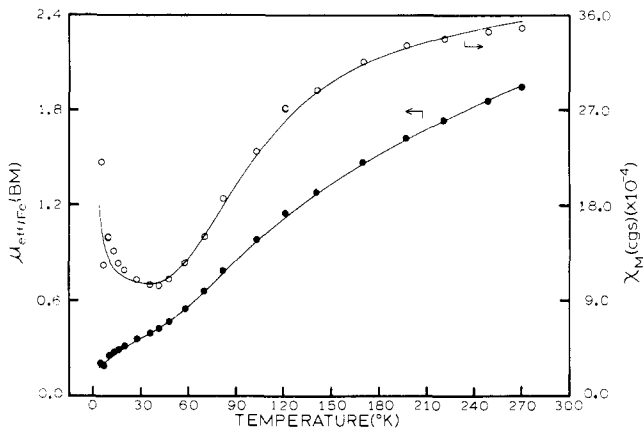


Figure 3. Temperature dependence of the magnetic susceptibility (open circles) and effective magnetic moments (solid circles) for $[\text{Cl}-\text{C}_7\text{H}_2\text{NO}_4(\text{H}_2\text{O})_2\text{Fe}]_2\text{O} \cdot 4\text{H}_2\text{O}$.

An improved fit was obtained with $-J = 107 \text{ cm}^{-1}$, TIP = 8.5 $\times 10^{-4} \text{ cgsu}$, and 0.08% of high-spin Fe(III) impurity. Magnetic moments calculated using the latter fitting procedure are presented in Table VI and in Figure 3. Corrections for the presence of high-spin Fe(III) impurities also were considered appropriate in the evaluation of J values for Fe_2O^{4+} complexes having Schiff bases²⁸ and heme⁵ groups as nonbridging ligands.

Our treatment of this dimer as a species for which $S_1 = S_2 = \frac{5}{2}$ is supported by (a) structural similarities (vide supra) with related $\text{Fe}_2(\text{OH})_2^{4+}$ dimers unambiguously containing $S = \frac{5}{2}$ Fe(III) ions and (b) spectral studies. Electronic-spectral features of the dimer include a weak ($\epsilon \approx 1$) band at $\sim 13\,000 \text{ cm}^{-1}$ (observable in pressed disks of the neat complex) and overlapping absorptions at $\sim 20\,400$ and $\sim 22\,200 \text{ cm}^{-1}$. These latter absorptions have ϵ values of ~ 30 for incident light parallel to the FeOFe direction in the crystals. Both the positions and intensities of the above absorption bands are reminiscent of those reported for Fe_2O^{4+} dimers having $S = \frac{5}{2}$ Fe(III) ions.⁴ Although magnetic susceptibility measurements alone cannot distinguish between Fe_2O^{4+} dimers of either $S = \frac{5}{2}$ or $S = \frac{3}{2}$ Fe(III) ions, only examples of the former type have been observed.⁴

Table VI. Magnetic Susceptibility Data for $[\text{Cl}-\text{C}_7\text{H}_2\text{NO}_4(\text{H}_2\text{O})_2\text{Fe}]_2\text{O} \cdot 4\text{H}_2\text{O}^a$

T, K	$10^3 \chi_m, \text{cgs}$		effective magnetic moment per Fe, μ_B	
	obsd	calcd	obsd	calcd
270.	3.39	3.48	1.91	1.94
249.	3.36	3.42	1.83	1.84
221.	3.29	3.32	1.70	1.71
197.	3.22	3.22	1.59	1.59
170.	3.06	3.05	1.44	1.44
141.	2.79	2.78	1.25	1.25
121.	2.62	2.51	1.12	1.10
103.	2.21	2.18	0.95	0.95
81.6	1.76	1.70	0.76	0.74
70.0	1.40	1.42	0.63	0.63
58.1	1.15	1.17	0.52	0.52
47.7	0.99	1.03	0.44	0.44
41.3	0.93	0.98	0.39	0.40
35.8	0.94	0.97	0.37	0.37
27.4	0.99	0.98	0.33	0.33
19.6	1.08	1.03	0.29	0.29
15.7	1.15	1.08	0.27	0.26
12.7	1.26	1.13	0.25	0.24
9.5	1.39	1.23	0.23	0.22
6.2	1.13	1.43	0.17	0.19
4.2	2.10	1.71	0.19	0.17

^a The diamagnetic correction used is $-350 \times 10^{-6} \text{ cgs}$ per dimer.

Superexchange pathways within a Fe_2O^{4+} unit consist of various orbital overlaps which serve to couple $S = \frac{5}{2}$ Fe(III) ions via the diamagnetic oxide bridge. Detailed considerations of these pathways suggest that linear Fe_2O^{4+} units with short Fe-O bond distances should show the largest antiferromagnetic coupling.⁷ In comparison with other oxo-bridged Fe(III) dimers of nonheme ligands,⁴ the title complex has (a) unremarkable Fe-O bond distances (1.772, 1.773 Å) which fall within the range typically observed (1.76–1.82 Å), and (b) a linear as opposed to bent (Fe-O-Fe = 139–178°) Fe_2O^{4+} unit. The extent of superexchange coupling in the title complex ($-J \approx 107 \text{ cm}^{-1}$) barely lies outside the range ($-J = 90$ –100 cm^{-1}) reported for the bent oxo-bridged Fe(III) species. It is

apparent that antiferromagnetic coupling within Fe_2O^{4+} units is not a very sensitive function of the Fe–O–Fe bridging angle. This result contrasts with the large angular dependence observed for $\text{Cu}_2(\text{OH})_2^{2+}$ units.²⁹ In view of this, the near linearity reported for the Fe_2O^{4+} units in two dimeric heme complexes⁵ cannot entirely account for the conspicuously large coupling ($-J = 122\text{--}146 \text{ cm}^{-1}$) characteristic of oxo-bridged heme dimers. Accordingly, we suggest that it originates from particularly tight Fe–O bonding. This suggestion is supported by several structural studies of monomeric and dimeric heme complexes containing $S = \frac{5}{2}$ Fe(III). The square pyramidal Fe(III) coordination geometry in such complexes has several peculiar structural features. The Fe(III) ions lie $\sim 0.5 \text{ \AA}$ from the best plane of the four porphyrin N donors and are displaced toward the fifth (apical) ligand. Moreover, the apical bond length is relatively short. For example, in chlorohemin,³⁰ the $\text{Fe}(S = \frac{5}{2})\text{-Cl(apical)}$ distance (2.218 \AA) was thought²⁴ to be more appropriate for $S = \frac{1}{2}$ Fe(III). However, subsequent crystallographic studies have shown that this distance is only slightly short for the type of bonding involved. The square pyramidal coordination geometry in chlorohemin is approximated by that of Fe(III)-chloro complexes with Schiff-base ligands; four such complexes have been studied crystallographically.^{31–33} Distances observed between the $S = \frac{5}{2}$ Fe(III) ions and the approximately apical Cl^- ions spanned the range $2.226\text{--}2.262 \text{ \AA}$. For comparison, a length of 2.314 \AA was reported for the Fe(III)-Cl bond in a six-coordinate high-spin complex of this type.³⁴ A length of 2.27 \AA was reported for the apical Fe–Cl bond of a square pyramidal complex of $S = \frac{3}{2}$ Fe(III) having an S_4Cl donor set; the Fe(III) was displaced 0.63 \AA from the best plane of the sulfur atoms toward the apical Cl ligand.³⁵ Simple high-spin six-coordinate Fe(III) complexes such as $(\text{NH}_4)_2\text{FeCl}_5\text{H}_2\text{O}$ exhibit Fe–Cl bond distances in the range $2.35\text{--}2.41 \text{ \AA}$.³⁶ Thus, an increase in coordination number from five to six results in a significant ($0.1\text{--}0.2 \text{ \AA}$) increase in the observed Fe–Cl bond lengths. From the above data, the Fe–Cl bond length observed for chlorohemin (2.218 \AA) is seen to be only a bit short relative to those for reference approximately square pyramidal $S = \frac{5}{2}$ Fe(III) complexes.

The apical Fe–O bond distance (1.842 \AA) reported for a $S = \frac{5}{2}$ methoxy Fe(III) heme derivative also appears short,²⁴ at least relative to Fe–O distances ($1.92\text{--}1.99 \text{ \AA}$) reported for various five- and six-coordinate hydroxo and alkoxo Fe(III) complexes.^{10,33,37} Coordination by the more nucleophilic phenoxy group present in various Schiff-base ligands^{31–33} results in Fe–O bond lengths in the range $1.85\text{--}1.91 \text{ \AA}$. Square pyramidal reference complexes of the type available for chlorohemin do not, to our knowledge, exist for the above methoxy Fe(III) heme complex.

Finally, we consider the oxo-bridged Fe(III) heme complexes, two of which have been characterized crystallographically. The shortest³⁸ Fe–O distance known to us ($\sim 1.73 \text{ \AA}$) is that reported for the Fe_2O^{4+} unit of μ -oxo-bis[protohemin dimethyl ester].⁵ A somewhat longer Fe–O bond distance (1.763 \AA) was reported for μ -oxo-bis[tetraphenylporphyrin iron(III)].⁶ Thus, these dimeric heme complexes exhibit Fe–O bond distances which are somewhat short compared with those ($1.76\text{--}1.82 \text{ \AA}$) of nonheme dimers of this type.⁴ Especially tight bonding may be anticipated within the Fe_2O^{4+} unit of dimeric heme complexes because both Fe–O bonds are apical components of square pyramidal $S = \frac{5}{2}$ Fe heme fragments. We believe that the strong coupling exhibited by such complexes more likely originates because of this structural feature and that the near linearity of the Fe_2O^{4+} units is of secondary magnetic significance. Some special electronic-structural role of the heme ligands apparently is also operable here since substantially less superexchange coupling occurs via two Fe–O bonds which are apical components of $S = \frac{5}{2}$ Fe Schiff-base

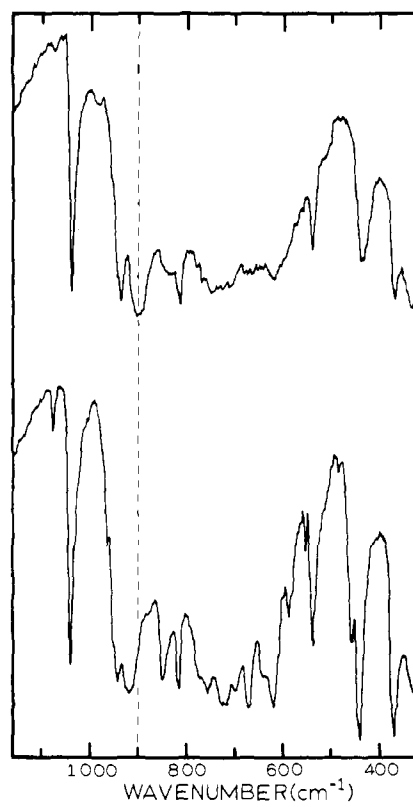


Figure 4. Infrared spectra at 300 (upper curve) and 30 K (lower curve) of $[Cl\text{-}C_7H_2NO_4(H_2O)_2Fe]_2O\cdot 4H_2O$ dispersed in a KBr pellet.

fragments. Structurally analogous to the oxo-bridged Fe(III) heme dimers, the Fe(III) ions in these latter complexes also are displaced $\sim 0.5 \text{ \AA}$ toward the apical oxide ions.

There is one other possible explanation for the apparently greater coupling in the oxo-bridged heme dimers. Iron(III) porphyrins are known to possess large, axial, single-iron, zero-field splittings (i.e., DS_z^2). For example, far-infrared measurements³⁹ on certain high-spin ferric porphyrins indicated zero-field splitting D values in the range of $5\text{--}17 \text{ cm}^{-1}$. The D values for nonporphyrin iron(III) complexes are expected to be considerably smaller. It has been our experience that the inclusion of the DS_z^2 term into the spin Hamiltonian could appreciably affect the exchange parameter obtained in the least-squares fitting of the data. Thus, the more negative J values evaluated for the oxo-bridged heme dimers could be an artifact of not accounting for the single-ion zero-field interactions.

Infrared Spectra

The antisymmetric stretching vibration, $\nu_{AS}(\text{Fe–O–Fe})$, is an infrared-active mode used to characterize oxo-bridged Fe(III) compounds.⁴ This strong characteristic absorption appears in the neighborhood of 850 cm^{-1} . Infrared absorption spectra were obtained at 300 and 30 K for the title complex and are shown in Figure 4. At 300 K in the region of $950\text{--}800 \text{ cm}^{-1}$, four absorptions occur at 936 , 902 (broad), 840 (unresolved), and 815 cm^{-1} . Decreasing the temperature to 30 K again results in four absorptions in this region. The 936 - and 815-cm^{-1} bands remain unchanged. However, the 902-cm^{-1} absorption shifts to 920 cm^{-1} and the 840-cm^{-1} absorption is resolved and shifted to 850 cm^{-1} . The only other changes in the two spectra are an increase of resolution in the region of $800\text{--}600 \text{ cm}^{-1}$ and an increase of intensity and resolution of the absorptions at 500 cm^{-1} . A single broad absorption at 436 cm^{-1} occurs at 300 K. At 30 K, this absorption is resolved into two absorptions, one

at 458 cm^{-1} and the other at 440 cm^{-1} which has increased in intensity with respect to the other bands in the spectrum.

Both the broad absorption at 902 cm^{-1} that shifts to 920 cm^{-1} at low temperatures and the absorption at 840 cm^{-1} that shifts to 850 cm^{-1} and becomes resolved are possible choices for the $\nu_{AS}(\text{Fe}-\text{O}-\text{Fe})$. Without an ^{18}O labeling experiment, it is not possible to assign either absorption unambiguously as the $\nu_{AS}(\text{Fe}-\text{O}-\text{Fe})$ mode. They may, in fact, be both attributable to the antisymmetric stretching mode. For example, $\nu_{AS}(\text{Fe}-\text{O}-\text{Fe})$ appears as a single absorption at 832 cm^{-1} for $\mu\text{-oxo-bis}(N,N'\text{-ethylenabis(salicylideneiminato)})\text{iron(III)}$ ²⁸ and as two absorptions at 870 and 890 cm^{-1} for $\mu\text{-oxo-bis(tetraphenylporphyrinato)}\text{iron(III)}$.⁴⁰ Thus, it is possible that the 180° $\text{Fe}-\text{O}-\text{Fe}$ angle in the title complex causes a splitting of the $\nu_{AS}(\text{Fe}-\text{O}-\text{Fe})$ which is even larger than that caused by the 174.5° $\text{Fe}-\text{O}-\text{Fe}$ angle in the oxo-bridged iron(III) porphyrin.

Further, we note that the two highest energy bands in Figure 4 also are exhibited⁴¹ by $[\text{Cl-C}_7\text{H}_2\text{NO}_4(\text{H}_2\text{O})(\text{OH})\text{Cr}]_2$, a dihydroxo-bridged⁴² Cr(III) analogue of the title complex. Additional infrared spectral coincidences suggest that the above two bands are ligand modes common to the similarly ligated Fe_2O^{4+} and $\text{Cr}_2(\text{OH})_2^{4+}$ units. Accordingly, it appears reasonable to associate the strong absorption at $\sim 902\text{ cm}^{-1}$ with the Fe_2O^{4+} unit. The relatively large blue shift of the 902- and 840-cm^{-1} bands at low temperatures is in agreement with the results of prior studies.⁴³

Acknowledgments. Research at Rutgers University was supported by the Rutgers Computing Center (H.J.S., J.A.P.), the Rutgers Research Council (H.J.S.), and a Rutgers Biological Science Support Grant (H.J.S.). Research at the University of Illinois was funded in part by National Institutes of Health Grant HL 13652.

Supplementary Material Available: Listing of structure factor amplitudes for the title complex (12 pages). Ordering information is given on any current masthead page.

References and Notes

- (1) (a) Rutgers University; (b) University of Illinois.
- (2) H. B. Gray and H. J. Schugar in "Inorganic Biochemistry", Vol. I, G. Eichhorn, Ed., American Elsevier, New York, N.Y., 1973, Chapter 3.
- (3) J. Webb in "Techniques and Topics in Bioinorganic Chemistry", C. A. McAuliffe, Ed., Wiley, New York, N.Y., 1975, Chapter 4.
- (4) K. S. Murray, *Coord. Chem. Rev.*, **12**, 1 (1974), and references cited therein.
- (5) D. H. O'Keefe, C. H. Barlow, G. A. Smythe, W. H. Fuchsman, T. H. Moss, H. R. Lilenthal, and W. S. Caughey, *Bioinorg. Chem.*, **5**, 125 (1975).
- (6) A. B. Hoffman, D. M. Collins, V. M. Day, E. B. Fleischer, T. S. Srivastava, and J. L. Hoard, *J. Am. Chem. Soc.*, **94**, 3620 (1972).
- (7) A. P. Ginsberg, *Inorg. Chim. Acta Rev.*, **5**, 45 (1971).
- (8) H. J. Schugar, A. T. Hubbard, F. Anson, and H. B. Gray, *J. Am. Chem. Soc.*, **91**, 71 (1969).
- (9) M. Cerdonio, F. Mogno, B. Pispisa, G. L. Romani, and S. Vitale, *Inorg. Chem.*, **16**, 400 (1977).
- (10) J. A. Thich, C. C. Ou, D. Powers, B. Vasiliou, D. Mastropaoletti, J. A. Potenza, and H. J. Schugar, *J. Am. Chem. Soc.*, **98**, 1425 (1976).
- (11) C. C. Ou, R. A. Lalancette, J. A. Potenza, and H. J. Schugar, *J. Am. Chem. Soc.*, **100**, 2053 (1978).
- (12) D. G. Markees and G. W. Kidder, *J. Am. Chem. Soc.*, **78**, 4130 (1956).
- (13) G. R. Hall and D. N. Hendrickson, *Inorg. Chem.*, **15**, 607 (1976).
- (14) J. P. Chandler, Program 66, Quantum Chemistry Program Exchange, Indiana University, Bloomington, Ind.
- (15) B. W. Low and F. M. Richards, *J. Am. Chem. Soc.*, **74**, 1660 (1952).
- (16) R. C. Weast, Ed., "Handbook of Chemistry and Physics", 53rd ed, Chemical Rubber Publishing Co., Cleveland, Ohio, 1972.
- (17) J. A. Thich, D. Mastropaoletti, J. Potenza, and H. J. Schugar, *J. Am. Chem. Soc.*, **96**, 726 (1974).
- (18) In addition to local programs for the IBM 360/67 computer, local modifications of the following programs were employed: Coppens's ABSORB program; Zalkin's FORDAP Fourier program; Johnson's ORTEP II thermal ellipsoid plotting program; Busing, Martin, and Levy's ORFFE error function and ORFLS least-squares program. The analysis of variance was carried out using program NANOVA obtained from Professor I. Bernal: see J. S. Ricci, Jr., C. A. Eggers, and I. Bernal, *Inorg. Chim. Acta*, **6**, 97 (1972).
- (19) D. T. Cromer and J. T. Waber, *Acta Crystallogr.*, **18**, 104 (1965).
- (20) "International Tables for X-Ray Crystallography", Vol. III, Kynoch Press, Birmingham, England, 1962, pp 201–213.
- (21) See paragraph at end of paper regarding supplementary material.
- (22) von E. Blasius and B. Brozio, *Ber. Bunsenges. Phys. Chem.*, **68**, 52 (1964).
- (23) A. Albert in "Physical Methods in Heterocyclic Chemistry", Vol. III, A. R. Katritzky, Ed., Academic Press, New York, N.Y., 1971, Chapter 9.
- (24) J. L. Hoard, M. J. Hamor, T. A. Hamor, and W. S. Caughey, *J. Am. Chem. Soc.*, **87**, 2312 (1965).
- (25) (a) *p*-Dichlorobenzene, 1.749 (3) Å, G. L. Wheeler and S. D. Colson, *Acta Crystallogr., Sect. B*, **31**, 911 (1975). (b) *(p*-Chlorophenyl)propionic acid, 1.741 (3) Å; *p*-chloro-*trans*-cinnamic acid, 1.747 (3) Å; J. P. Glusker, D. E. Zacharias and H. L. Carroll, *J. Chem. Soc., Perkins Trans. 2*, 68 (1975).
- (c) 2,2'-Dichlorobiphenyl, 1.741 (3) Å, C. Romming, H. M. Seip, and I.-M. Aanesen Øymo, *Acta Chem. Scand., Ser. A*, **28**, 507 (1974).
- (26) A. Earnshaw, "Magnetochemistry", Academic Press, New York, N.Y., 1969.
- (27) W. Wojciechowski, *Inorg. Chim. Acta*, **1**, 319 (1967).
- (28) R. G. Wollmann and D. N. Hendrickson, *Inorg. Chem.*, **16**, 723 (1977).
- (29) V. H. Crawford, H. W. Richardson, J. R. Wasson, D. J. Hodgson, and W. E. Hatfield, *Inorg. Chem.*, **15**, 2107 (1976).
- (30) D. F. Koenig, *Acta Crystallogr.*, **18**, 663 (1965).
- (31) M. Gerloch and F. E. Mabbs, *J. Chem. Soc. A*, 1598 (1967).
- (32) J. E. Davies and B. M. Gatehouse, *Chem. Commun.*, 1166 (1970).
- (33) J. A. Bertrand, J. L. Breece and P. G. Eller, *Inorg. Chem.*, **13**, 125 (1974).
- (34) J. A. Bertrand and J. L. Breece, *Inorg. Chim. Acta*, **8**, 267 (1974).
- (35) R. L. Martin and A. H. White, *Inorg. Chem.*, **6**, 712 (1967).
- (36) *Struct. Rep.*, **11**, 417 (1951). Magnetic susceptibility studies of $(\text{NH}_4)_2[\text{FeCl}_5(\text{H}_2\text{O})]$ show that it is a $S = \frac{5}{2}$ Fe(III) complex. See E. Konig in "Magnetic Properties of Coordination and Organo-Metallic Compounds", Vol. II, New Series of Landolt-Bornstein, K. H. Hellwege, Ed., Springer-Verlag, West Berlin, 1966, Chapter 2, p 116.
- (37) J. A. Bertrand and P. G. Eller, *Inorg. Chem.*, **13**, 927 (1974).
- (38) The precision of this bond distance is uncertain because of crystallographic difficulties. Refinement of the atom positions was not completed because of disordering of the heme vinyl groups and the consequent expense of further refinement (private communication from J. L. Hoard).
- (39) W. S. Caughey, H. Eberspaecher, W. H. Fuchsman, and S. McCoy, *Ann. N.Y. Acad. Sci.*, **153**, 722 (1969).
- (40) I. A. Cohen, *J. Am. Chem. Soc.*, **91**, 1980 (1969).
- (41) C. C. Ou, unpublished results.
- (42) Private communication from Derek Hodgson.
- (43) H. J. Schugar, G. R. Rossman, C. G. Barracough, and H. B. Gray, *J. Am. Chem. Soc.*, **94**, 2683 (1972), and references cited therein.